

Fusion Zone Grain Refinement in Aluminum Alloy Welds through Magnetic Arc Oscillation and Its Effect on Tensile Behavior

G.D. Janaki Ram, R. Murugesan, and S. Sundaresan

(Submitted 11 September 1998; in revised form 6 April 1999)

Grain size reduction in weld fusion zones confers the advantages of an increased resistance to solidification cracking and an improvement in mechanical properties. Oscillation of the welding arc through an imposed alternating magnetic field is one of several approaches to modify weld solidification structures. In this study, gas tungsten arc welds were produced in two high strength, age hardenable aluminum alloys with and without an external magnetic field. Metallographic characterization revealed the degree of structural refinement produced by magnetic arc oscillation. The decrease in grain size was found to increase tensile elongation, while the effect on strength and age hardening response was only meager. The improvement in ductility was partially maintained in the peak aged condition also.

Keywords aluminum alloys, grain refinement, welding

1. Introduction

The formation of fine equiaxed grains in weld fusion zones helps in reducing solidification cracking and in improving the mechanical properties of the weld metal including ductility, fracture toughness, and fatigue life (Ref 1, 2). While in relation to castings, grain refinement techniques are seldom practiced in the welding industry, many methods for controlling the grain structure in weld metals have been reported in literature. These include inoculation by the use of grain refining agents, vibration of the welding torch, current pulsation, and magnetic arc oscillation (Ref 2).

If the natural convection existing in the weld pool could be enhanced by artificial agitation, advantages in terms of grain refinement could be realized. One method of inducing such disturbance is to cause the welding arc to oscillate by using an alternating external magnetic field. It is well known that the interaction of the arc current and its own magnetic field leads to Lorentz forces that cause fluid flow and a self-induced stirring effect, particularly when the current density is large. Reinforcing the natural flow with an external magnetic field enhances this effect. The forces on the arc due to the external field depend on their relative orientation. If the field is coaxial with the arc, the induced forces will be perpendicular to both the magnetic field and the radial component of the diverging current through the arc. This will result in the rotation of the arc and in an annular flow of the molten metal in the weld pool. The flow will be reversed periodically if an alternating magnetic field is used, thus leading to electromagnetic stirring (EMS). In the situation where the external magnetic field is oriented parallel to the welding direction, the interaction of this alternating field with

the axial component of the diverging arc current results in an oscillation of the arc in the plane of the sheet transverse to the welding direction, referred to hereafter as magnetic arc oscillation (MAO).

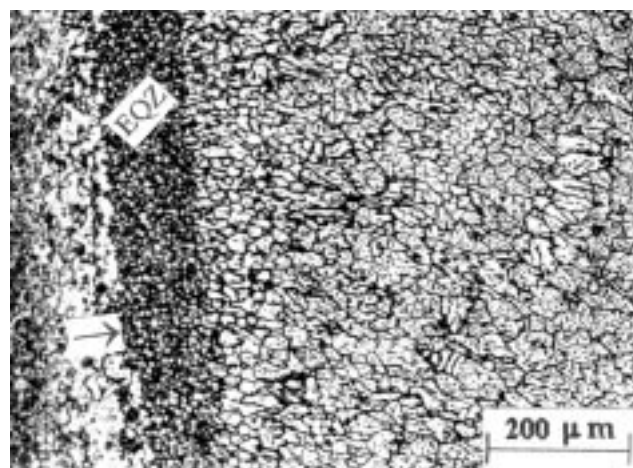
Brown et al. (Ref 3) were among the earliest to investigate the effects of EMS and to observe grain refinement in stainless steels, titanium, and aluminum alloys. Early Russian work demonstrated the usefulness of applied magnetic fields and, indeed, equipment appears to have been developed for industrial application (Ref 4). Tseng and Savage (Ref 5) refined the solidification substructure and decreased hot cracking tendency in high tensile steel weld metal. The effectiveness of applied magnetic fields in reducing weld metal grain size has been demonstrated in several materials, for example, austenitic stainless steel (Ref 6), titanium alloys (Ref 7, 8), tantalum (Ref 9), and iridium (Ref 10).

Following early work by Garland (Ref 11), who observed grain refinement in aluminum-magnesium alloy gas tungsten arc welds (GTAWs) through vibration of the welding torch, many reports have appeared concerning the effect of external magnetic fields on aluminum alloy welds. Matsuda et al. (Ref 12, 13) have extensively studied the effects of EMS in various aluminum alloys. They found that, at optimum frequency and amplitude, EMS significantly refines the solidification structure, reduces the occurrence of defects, and homogenizes the composition of the weld metal. According to their research, the effectiveness of grain refinement is most marked in alloys of long freezing range. Similarly, MAO has been successfully used to induce grain refinement and improve weld metal properties in an aluminum-lithium alloy (Ref 14) and in an aluminum-magnesium alloy (Ref 15). The combined treatment of heterogeneous nucleation and EMS has been used by many investigators to obtain significant grain refinement in various aluminum alloys (Ref 1, 16).

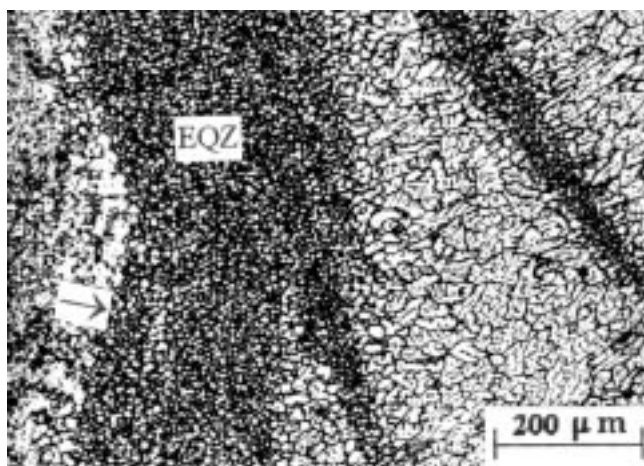
Though many previous studies have thus addressed the problem, the reported effects of arc oscillation on weld metal grain refinement have not been consistent. For example, Boldyrev (Ref 7) found that, while EMS refines titanium alloy

G.D. Janaki Ram, R. Murugesan, and S. Sundaresan, Department of Metallurgical Engineering, Indian Institute of Technology, Madras 600 036, India. Contact S. Sundaresan at e-mail: sandy@iitm.ernet.in.

welds, the effect was less than in austenitic stainless steel welds. Conversely, DeNale and Lukens (Ref 17) observed that a transverse magnetic field had little effect on the fusion zone grain structure in titanium alloy GTAWs. Transverse and longitudinal arc oscillations were found to have no effect on aluminum alloys (Ref 18) and steel (Ref 5) GTAWs, while grain refinement due to arc oscillation was successfully demonstrated in aluminum-magnesium alloy welds (Ref 11-15). Furthermore, different investigators have put forward different mechanisms to explain any observed grain refinement, ranging from heterogeneous nucleation (Ref 3) to dendrite breakup (Ref 12) and grain detachment (Ref 16). Also, while many studies have been conducted on weld metal grain refinement, and it has been suggested that such refinement could improve mechanical properties (Ref 1, 2), very few investigators have determined these properties and established a correlation with the structural refinement observed. In the current paper, therefore, an effort has been made to use MAO for reducing the fusion zone grain size in two aluminum alloys and to relate it to the tensile properties of the fusion zone.



(a)



(b)

Fig. 1 Fusion zone in 2090 (L-B section) region near fusion line. Arrows indicate fusion boundary. EQZ, nondendritic equiaxed zone. (a) Unoscillated. (b) Oscillated

2. Experimental Procedures

Two materials were investigated: an Al-Li-Cu alloy corresponding to 2090-T3 and an Al-Zn-Mg alloy corresponding to 7020-T6. Both were in the form of 3.2 mm thick sheet. The compositions were as follows: 2090-Al-2.6%Cu-2.2%Li-0.15%Zr and 7020-Al-4.2%Zn-1.2%Mg-0.15%Zr.

Gas tungsten arc welding was used to deposit autogenous, full penetration, bead-on-plate welds. The welds were made in a fully automatic GTAW machine with an attachment of commercially available electromagnetic arc oscillation equipment. This consists of a water-cooled electromagnetic probe that mounts on to the welding torch and a control unit. Suitable controls are provided to permit independent adjustment of the frequency and the amplitude of the square-wave current signal and, hence, of the alternating magnetic field. Preliminary trials were conducted at different arc oscillation amplitudes ranging from 0.2 to 0.8 mm. These tests established that an amplitude of 0.6 mm was most effective without other adverse effects. At lower amplitudes (lower field intensities) the structural refinement was not appreciable, while at higher amplitudes the arc behavior was erratic, leading to bead roughness and burn through. Welds were then deposited at frequencies of 1, 2.5, 5, 7.5, 10, and 20 Hz, keeping the amplitude constant at 0.6 mm. Subsequent microscopic examination showed that frequencies of 7.5 Hz and greater had little beneficial influence. Noticeable grain refinement was observed only at the lower frequencies. Here, closer examination showed that the grain refinement effect was highest at a frequency of 2.5 Hz, for both the materials studied. All the oscillated welds (with alternating external magnetic field) reported in this work were produced at an amplitude of 0.6 mm and a frequency of 2.5 Hz. For comparison, welds were also made without magnetic arc oscillation. Before welding the 2090 alloy, the sheet coupons were machined to remove adequate surface material for avoiding porosity that is known to result otherwise (Ref 19). Table 1 gives the welding conditions.

For metallographic specimen preparation a solution of 8 mL HNO₃, 5 mL HCl, and 3 mL HF in water was used for an etchant. At least two mutually perpendicular sections of the fusion zone were examined for a clear understanding of the microstructural features.

Because both alloys are age hardenable, it would be of interest to see if the aging behavior is influenced by MAO. Preliminary aging studies were conducted to establish optimum postweld treatment parameters for both 2090 and 7020 alloys. In the former case, it was found that without a solution treatment after welding the hardness pickup during aging was not appreciable. The solution treatment and aging temperatures were taken from literature as 540 and 160 °C, respectively. It

Table 1 Welding and arc oscillation parameters

Parameters	Value
Arc voltage	12 V
Arc current	125 A
Travel speed	240 mm/min
Magnetic oscillation amplitude	0.2, 0.4, 0.6, 0.8 mm
Magnetic oscillation frequency	1, 2.5, 5, 7.5, 10, 20 Hz

was also found that cold working following solution treatment led to a considerable increase in the hardening during subsequent aging, due to the increase in dislocation density and, hence, the number of nucleation sites for precipitation. A strain of 5% was shown to be optimum in this regard. Thus the best aging response in the 2090 alloy was obtained by solution treatment (540 °C for ½ h) followed by cold work (5%) and aging (160 °C). For the 7020 alloy, conversely, it was found that solution treatment after welding was not necessary and that straining did not produce any additional benefit. Two aging schedules were tried: single-step aging at 120 °C and double-step treatment at 100 °C for 8 h followed by aging at 150 °C. This study showed that there was no additional improvement in peak hardness due to the two-step treatment over the one-step treatment. For the 7020 alloy, therefore, a simple aging schedule at 120 °C was adopted following welding. Fusion zone samples from both the alloys were given these respective optimized treatments. In both cases the peak hardness was reached in 36 h.

It was considered likely that any observed grain refinement might improve the tensile properties. Longitudinal all-weld

specimens were machined from the weldments corresponding to ASTM E 8M. Testing was done in a 2 tonne Hounsfield tensometer at a crosshead travel speed of 0.5 mm/min.

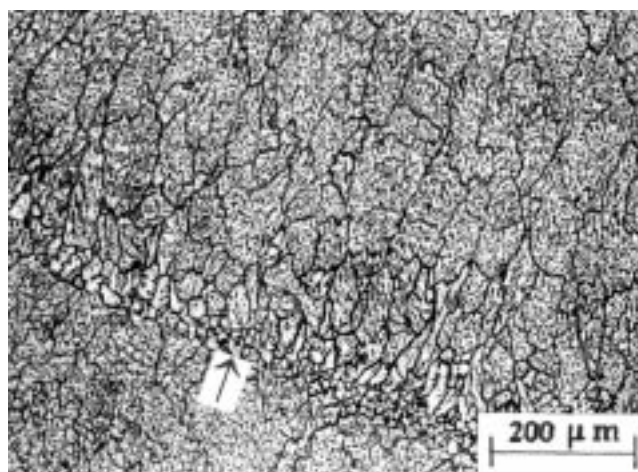
3. Results and Discussion

3.1 Microstructures

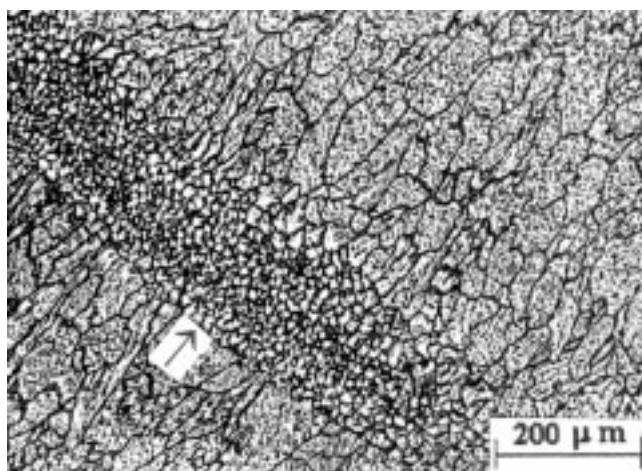
The micrographs of the top (L-B) sections of the fusion zone in the unoscillated (without external magnetic field) and magnetically oscillated welds in the 2090 alloy are shown in Fig. 1 near the fusion boundary and in Fig. 2 toward the center of the weld. Three important features emerge from these microstructures: a zone of fine equiaxed grains adjacent to the fusion line that are nonepitaxial and exhibit no sign of any dendritic growth, columnar dendrites in the weld interior, and bands of fine equiaxed grains looping across the weld from one fusion boundary toward the other.

The fine-grained zone parallel to and adjacent to the fusion boundary has sometimes been called the chill zone (Ref 14) or the nondendritic equiaxed zone (EQZ) (Ref 20) and is believed to arise as follows. Prior to welding, the thermomechanically processed base material contains dispersoid particles comprised of Al_3Zr and $Al_3(Li, Zr)$. The heat of welding normally dissolves these particles, but in a narrow region adjacent to the fusion boundary they survive without melting. The thermal and fluid flow conditions in this region are such that the particles are neither dissolved nor swept into the bulk of the weld pool (Ref 20). The fine grains in the EQZ arise by heterogeneous nucleation on these dispersoid particles.

Comparing the unoscillated and oscillated weld microstructures in Fig. 1 and 2, it is seen that MAO has widened the chill zone at the fusion line (Fig. 1) and has also resulted in relatively wide bands of fine grains forming across the weld (Fig. 2b). The bands are nearly regularly spaced along the length of the weld. At some places these fine-grained bands are particularly wide. One such region is shown in Fig. 3, taken from the L-B section of an oscillated weld. In contrast, though the unoscillated weld shows occasional stray bands such as the band in



(a)



(b)

Fig. 2 Fusion zone in 2090 (L-B section) near weld center. Arrows indicate fine-grained bands. (a) Unoscillated. (b) Oscillated

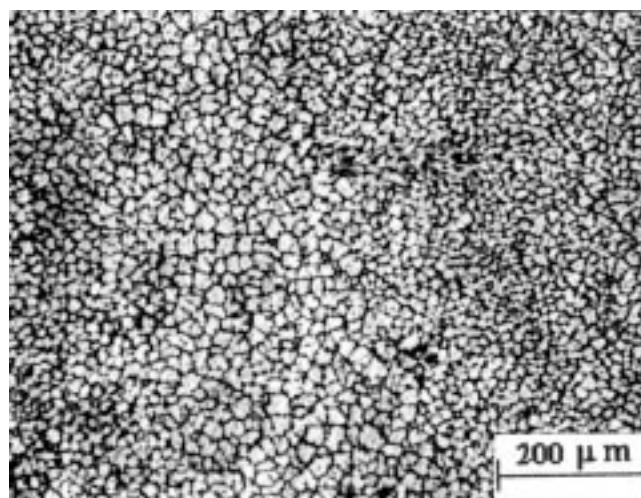


Fig. 3 Fusion zone in 2090 oscillated weld (L-B section) showing wide fine-grained band in the weld interior

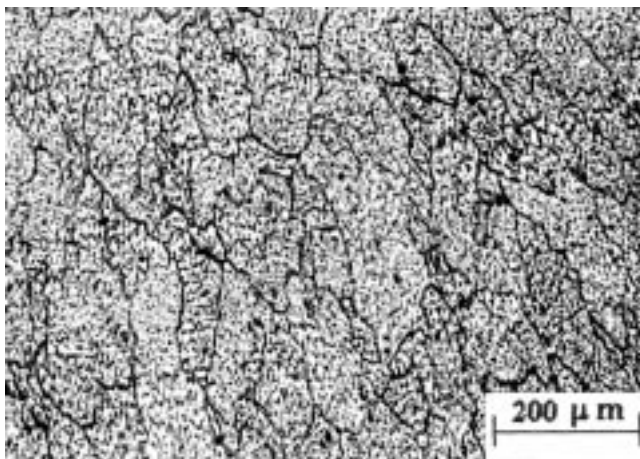
Fig. 2(a), these are narrow and occur at random locations. A reduction in the grain size in the columnar dendrites in the weld interior due to MAO is also apparent in these micrographs. However, this distinction is more clearly noticeable in Fig. 4(a) and (b), taken from the longitudinal or L-T section in the fusion zone. The oscillated weld shows a mixture of columnar and equiaxed grains, while the unoscillated weld shows predominantly columnar grains of much larger size. All these micrographs thus show that MAO results in considerable refinement of the solidification structure, with the average grain size being much smaller than in the unoscillated weld.

The micrographs of the unoscillated and oscillated welds in the weld fusion zones of the 7020 alloy were qualitatively similar to those in the 2090 alloy. For example, the columnar dendrites in the weld interior are shown in Fig. 5, taken from the top or L-B section and Fig. 6, taken from the transverse or B-T section. These photographs clearly demonstrate the grain refining effect of MAO in the 7020 alloy also. Figures 7(a) and (b) show the microstructures close to the fusion boundary. The occurrence of a zone with nondendritic equiaxed grains is clearly seen in the oscillated weld (Fig. 7b). In the unoscillated weld

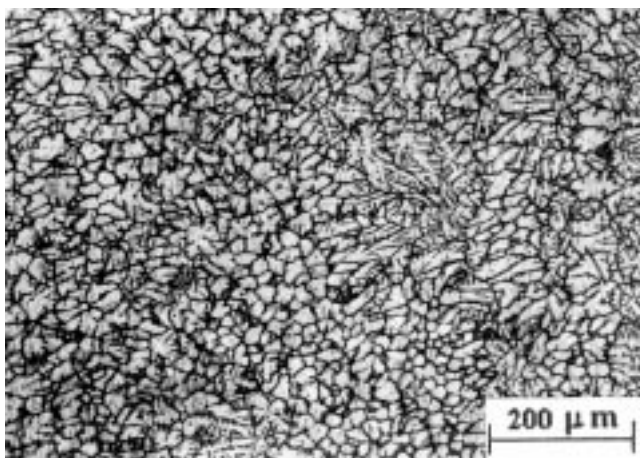
(Fig. 7a), this zone is seen to form, but is much narrower and much less distinct. All available information in literature on the formation of EQZ pertains only to weldments in the zirconium containing, aluminum-lithium alloys. Figure 7(a) and more clearly Fig. 7(b) demonstrate that such zones can form under favorable circumstances in the autogenous 7020 weldments also. Because this alloy also contains zirconium, it is presumed that the occurrence of the EQZ is due to heterogeneous nucleation on the Al_3Zr particles available in the alloy.

As in the 2090 alloy, bands of equiaxed grains occur in 7020 also, interspersed with columnar grains along the length of the weld. These are shown in Fig. 8(a) and (b). It can be noted that the stray band in the unoscillated weld is quite narrow in relation to the wider and more frequently occurring bands in the oscillated weld.

To illustrate quantitatively the reduction in grain size caused by MAO, the average grain sizes were measured and are presented in Table 2. These measurements were made in two mutually perpendicular sections near the center of the weld in both the alloys studied. Grain sizes are smaller in the B-T section than in the L-B section because of the geometry of the growth

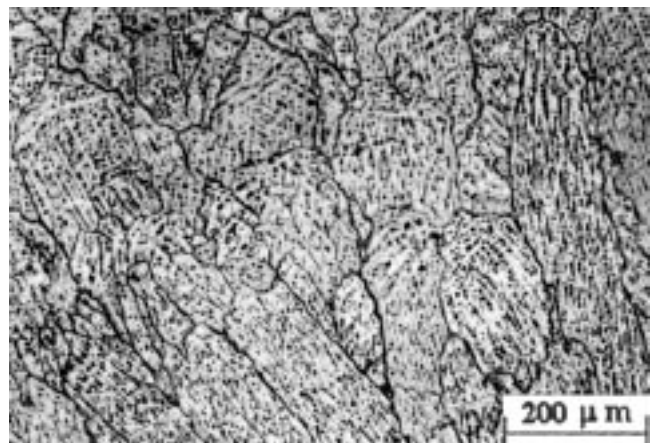


(a)

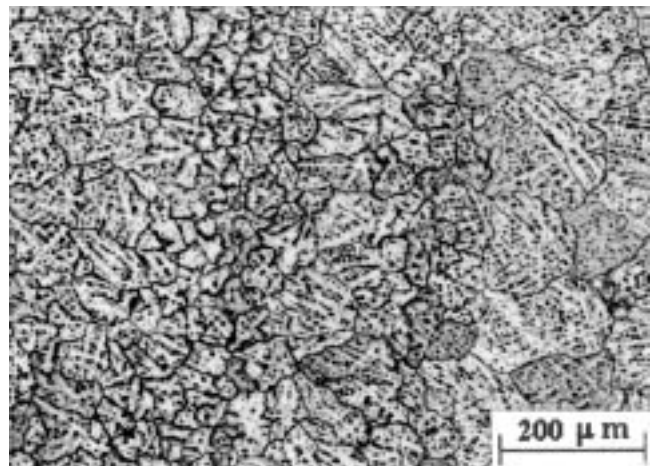


(b)

Fig. 4 Fusion zone in 2090 weld interior (L-T section). (a) Unoscillated. (b) Oscillated



(a)



(b)

Fig. 5 Fusion zone in 7020 weld interior (L-B section). (a) Unoscillated. (b) Oscillated

process in the weld fusion zone. Importantly, however, there is a considerable reduction in grain size in all three directions due to magnetic oscillation.

Many features of weld metal solidification are influenced by MAO. The forces due to the external magnetic field augment the indigenous Lorentz forces in the weld pool and thus increase fluid flow and reduce temperature gradients. In addition, the arc oscillation changes the shape of the weld pool continuously, and thus the direction of maximum thermal gradient at the solidifying boundary also changes with time. This leads to a situation in which, instead of a few favorably oriented grains growing over long distances, newer grains become favorably oriented with respect to the instantaneous direction of maximum thermal gradient leading to grain refinement (Ref 14).

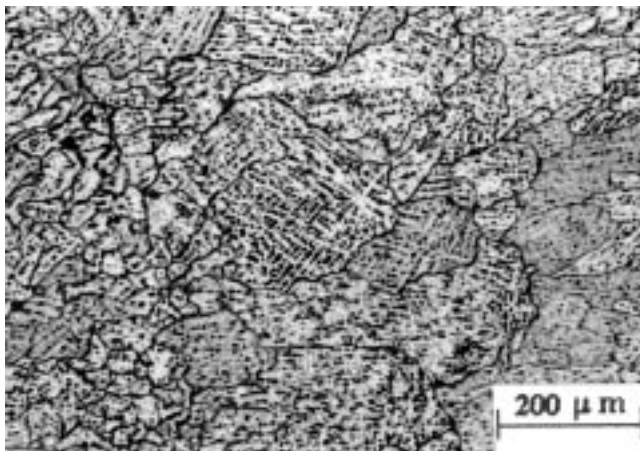
According to Kou and Le (Ref 1) oscillation can induce grain refinement in three possible ways: (a) dendrite fragmentation at the rear end of the weld pool, (b) detachment of partially melted grains from both sides of the weld puddle, and (c) heterogeneous nucleation. The enhanced fluid flow due to MAO helps in transferring the dendrite bits, detached grains, and heterogeneous nuclei to the region of constitutional supercooling just ahead of the solid-liquid interface. The lowering of

thermal gradients due to MAO makes all three kinds of nuclei more effective by prolonging their survival.

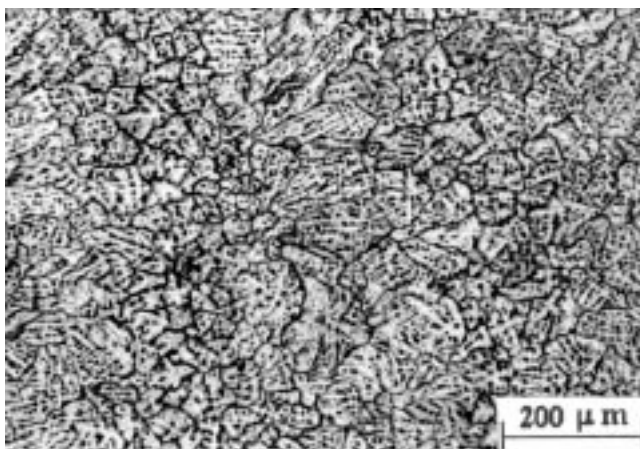
In their own study on 6061 alloy GTA welds, Kou and Le (Ref 1) used an overlap welding technique to demonstrate that heterogeneous nucleation was the mechanism by which MAO produced the observed grain refinement. Pearce and Kerr (Ref 16) also used an overlap welding technique in the GTA welding of several aluminum alloys to show that (a) heterogeneous nucleation was the dominant mechanism in the presence of titanium and (b) grain detachment at the fusion boundary could occur in the absence of heterogeneous nuclei.

Table 2 Average fusion zone grain sizes

Alloy	Section	Average grain size, μm	
		Unoscillated	Oscillated
2090	L-B	89	33
	L-T	82	30
7020	L-B	108	42
	B-T	72	30

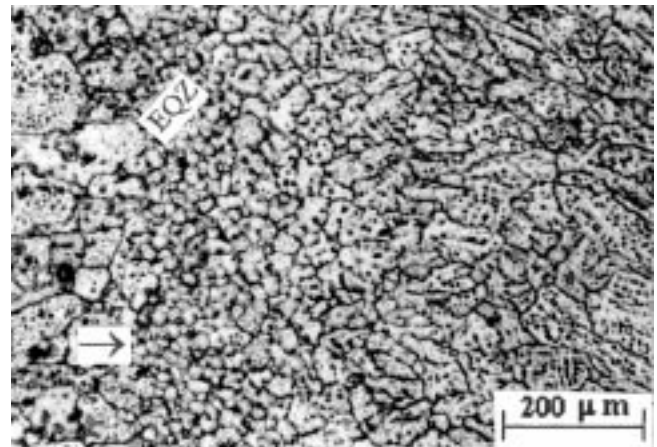


(a)

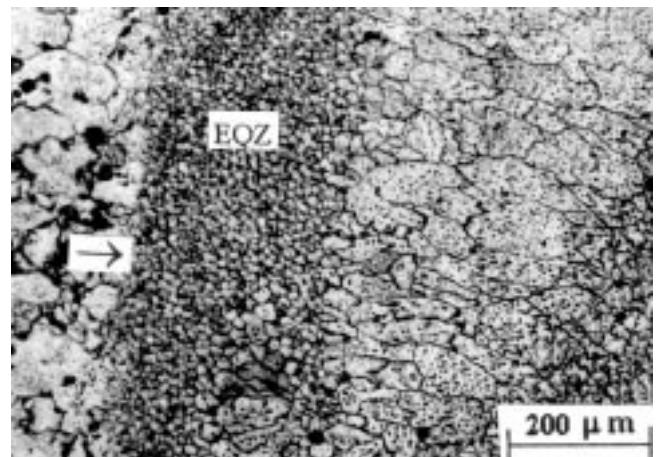


(b)

Fig. 6 Fusion zone in 7020 weld interior (B-T section). (a) Unoscillated. (b) Oscillated



(a)



(b)

Fig. 7 Fusion zone in 7020 (L-B section), region near fusion line. Arrows indicate fusion boundary. EQZ, nondendritic equiaxed zone. (a) Unoscillated. (b) Oscillated

It is important to note that, while dendrite fragmentation has frequently been cited as a possible mechanism, it has never been demonstrated to be operative. It has been sometimes suggested that the mechanism of dendrite breakup may not be effective in welding because of the small size of the fusion welds (Ref 2) and the fine interdendritic spacing in the weld microstructure (Ref 10, 16). Thus, while arc oscillation undoubtedly enhances fluid flow, the penetration of the fluid motion into such a dendrite network might be very difficult.

The grain refinement observed in the current investigation is therefore believed to be more due to the other effects of MAO on the weld pool shape, fluid flow, and thermal gradients. The continual change in the weld pool shape due to MAO is considered to be responsible for the reduction in columnar grain size in the interior of the fusion zone. As the direction of maximum thermal gradient is altered continuously, newer grains successively become favorably oriented. Thus, while each grain grows only a small distance, more grains grow resulting in a finer grain structure.

The arc oscillation has also resulted in two other important microstructural effects, a widening of the chill zone adjacent to the fusion boundary and the generation of fine-grained bands

distributed along the length of the weld. Regarding the former, the reduction of thermal gradients due to MAO can be expected to widen the region over which the nucleant particles survive. Thus the heterogeneous nucleation on these particles occurs over a larger area. The occurrence of fine-grained bands in the interior of the oscillated welds can be explained also in terms of differences in nuclei dissolution. In the unoscillated welds these nucleant particles might not survive the higher temperatures that are continuously maintained all along the center of the pool. In the oscillated weld, conversely, the weld pool becomes wider, fluid flow is enhanced, and thermal gradients are reduced. Additionally, the simultaneous to-and-fro and forward movements of the arc result in regions in the weld pool in which the superheating effect is less than in other regions. The nucleant particles are better able to survive in these regions of relatively lower temperature, and the chill zone from the fusion boundary can then extend into these regions. The bands occur with a fairly regular spacing between them because of the periodic reversal of the arc motion.

As in several other investigations (Ref 12, 16) an optimum combination of amplitude and frequency of arc oscillation was found to yield the best results. The reason for using the 0.6 mm amplitude has previously been explained. Regarding frequency, it is apparent that at very low frequencies the physical disturbance of the weld pool is not adequately intense. At frequencies higher than the optimum, conversely, less time is available during a half-cycle before the direction of fluid flow is reversed; the agitated liquid is then able to achieve only a lower velocity, thus reducing the effectiveness of the magnetic field (Ref 16).

3.2 Tensile Properties

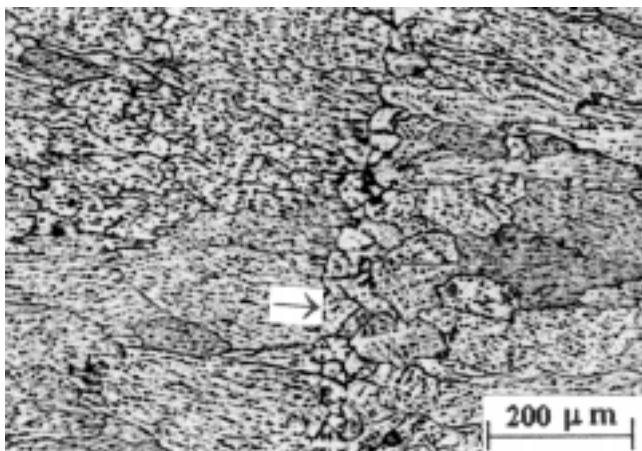
Table 3 lists the weld metal tensile properties. As mentioned earlier, these were determined from longitudinal all-weld tensile specimens taken from the fusion zone.

As-Welded Condition. The refinement of the solidification structure is seen to have exercised little effect on the yield and tensile strengths of the 2090 welds, while there is a slight increase in these in the 7020 alloy. More importantly, however, tensile ductility has been appreciably improved by the grain refinement in both alloys. This is not surprising because, while a finer grain size is known to improve ductility at all levels, its contribution to an increase in strength is marked only for very fine grain sizes (typically less than or equal to 5 μm) (Ref 21).

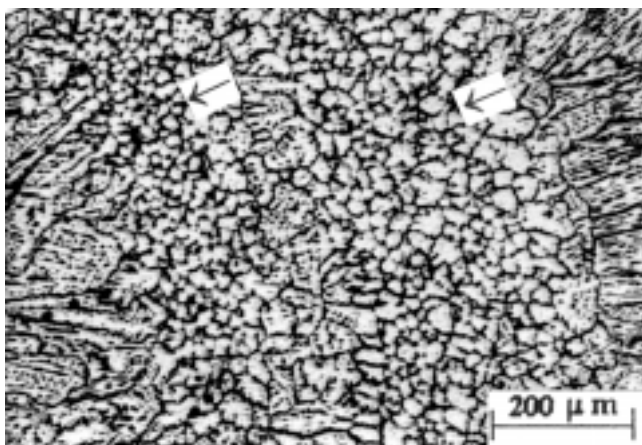
This difference in tensile behavior is also demonstrated in the scanning electron micrographs of the tensile fracture faces shown in Fig. 9 and 10. In the unoscillated condition in both the alloys (Fig. 9a and 10a), though ductile fracture features such as tear ridges and some dimples are seen, a few areas of flat fracture can also be observed. The oscillated welds, conversely, show deep, predominantly equiaxed dimples, indicative of a higher fracture strain; there is no evidence of any cleavage fracture.

Postweld Aged Condition. Aging studies conducted on samples from the weld fusion zones showed that there was only a slight increase in the age-hardening response due to the observed grain refinement in both the materials investigated.

Longitudinal tensile specimens prepared from weld metals (length along the welding direction) were also aged to peak



(a)



(b)

Fig. 8 Fusion zone in 7020 (L-B section) near weld center. Arrows indicate fine-grained bands. (a) Unoscillated. (b) Oscillated

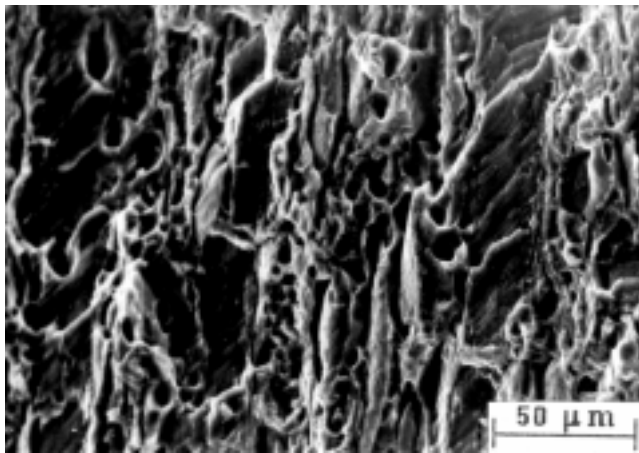
hardness according to the schedules already described. Table 3 lists the results of tensile testing in the postweld aged condition. In all four cases, as expected, the aging treatment increased the yield and tensile strengths and reduced tensile elongation. A comparison of the unoscillated and oscillated welds shows that, in the postweld aged condition also, the oscillated welds possess a higher ductility. The strength values are also higher, but only slightly.

Compared with the base material tensile properties also listed in Table 3, it is seen that, in case of the 7020 alloy, the weld strengths are only slightly different from those in the base material, while the ductility is much reduced. This is obviously due to the relatively large grain size in the weld fusion zone and possibly also due to interdendritic segregation effects. For the 2090 alloy, conversely, there is an appreciable reduction in the yield and tensile strengths of the weld in comparison to the base

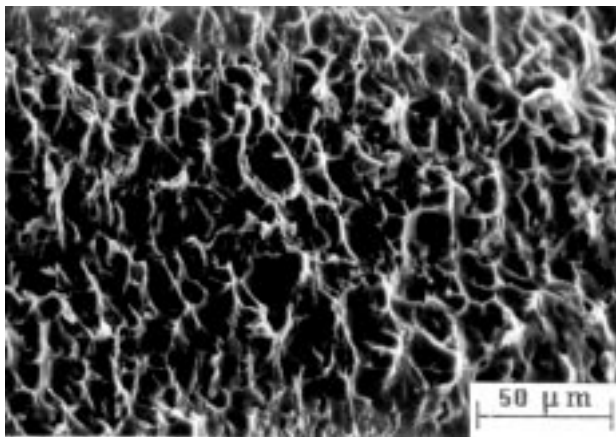
Table 3 Base metal and fusion zone tensile properties

Condition	As-welded			Postweld age hardened		
	0.2% proof stress, MPa	Ultimate tensile strength, MPa	Elongation, %	0.2% proof stress, MPa	Ultimate tensile strength, MPa	Elongation, %
2090-T3(a)						
Fusion zone, unoscillated	179	221	8.9	272	334	4.3
Fusion zone, oscillated, 0.6 mm, 2.5 Hz	176	227	12.6	284	348	5.8
7020-T6(b)						
Fusion zone, unoscillated	218	257	6.7	322	362	3.0
Fusion zone, oscillated, 0.6 mm, 2.5 Hz	236	275	10.4	326	376	4.2

Each set of tensile data is an average of measurements on three specimens. (a) Base metal: 0.2% proof stress, 375 MPa; ultimate tensile strength, 450 MPa; elongation 5.5%. (b) Base metal: 0.2% proof stress, 317 MPa; ultimate tensile strength, 383 MPa; elongation 12.2%

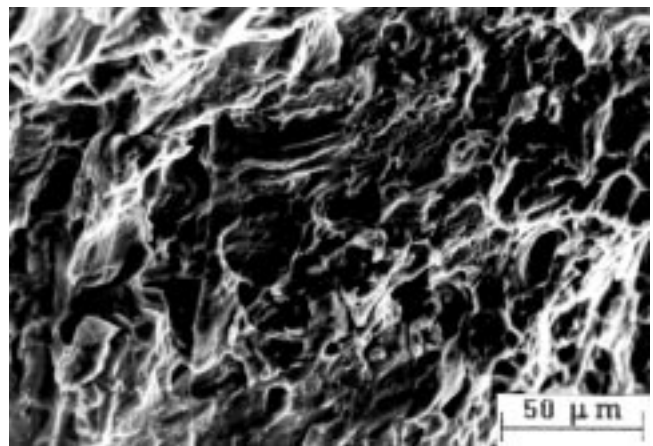


(a)

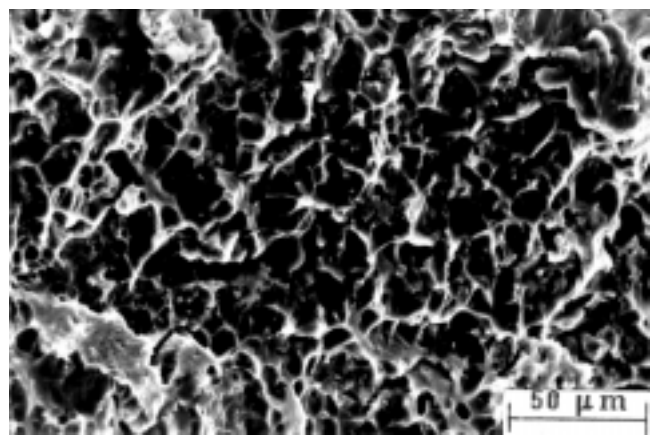


(b)

Fig. 9 Scanning electron microscopy fractographs of 2090 tensile fracture faces. (a) Unoscillated. (b) Oscillated



(a)



(b)

Fig. 10 Scanning electron microscopy fractographs of 7020 tensile fracture faces. (a) Unoscillated. (b) Oscillated

material. Such a loss of strength in the fusion zone was also noticed in an earlier investigation on welded aluminum-lithium alloys (Ref 22). The presence of zirconium in the thermomechanically processed 2090 alloy results in the formation of dispersoid particles that stabilize a fine subgrain structure during processing. This contributes substantially to the strengthening of the base material. The strength of the weld is lower than that of the base material, primarily due to the loss of such substructure strengthening during welding. It should also be noted that the dispersoid particles may undergo partial dissolution during welding and cannot reprecipitate, due to the rapid cooling involved in welding (Ref 23). The consequent reduction in the dispersion hardening effect due to these particles may also have contributed to the loss of strength in the weld metal.

4. Conclusions

The following conclusions can be drawn:

- Transverse magnetic arc oscillation at optimum amplitude and frequency leads to significant grain refinement in the two alloys studied.
- A nonepitaxial, nondendritic, equiaxed zone is produced next to the fusion boundary in both the 2090 and 7020 alloys and becomes wider in oscillated welds.
- The reduction in average grain size improves tensile ductility appreciably, but has little effect on the strength or the aging response.
- The improvement in tensile elongation is partially maintained in the peak-aged condition also.
- In relation to the base metal, there is a considerable loss of strength in the 2090 weld metal in the aged condition, which is attributed to the loss of substructure strengthening. The loss of some dispersion hardening may also play a role.

References

1. S. Kou and Y. Le, *Weld. J.*, Vol 65, 1986, p 305s-313s
2. S. Kou, *Proc. Conf. on Recent Trends in Welding Science and Technology* (Gatlinburg, Tennessee), S.A. David and J.M. Vitek, Ed., 1989, p 137-146
3. O.C. Brown, F.A. Crossley, J.F. Rudy, and H. Schwartzbart, *Weld. J.*, Vol 41, 1962, p 241s-250s
4. G.J. Davies and J.G. Garland, *Int. Met. Rev.*, Vol 20, 1975, p 83-105
5. C.F. Tseng and W.F. Savage, *Weld. J.*, Vol 50, 1971, p 777-785
6. T. Watanabe, H. Nakamura, and K. Ei, *Trans. Jpn. Weld. Soc.*, Vol 21, 1990, p 37-43
7. A.M. Boldyrev, E.B. Dorofeev, and E.G. Antonov, *Weld. Prod.*, Vol 18, 1971, p 54-58
8. V.E. Blashchuk, L.M. Onoprienko, G.M. Shelenkov, and V.E. Troyanovskii, *Weld. Prod.*, Vol 35, 1982, p 35-37
9. Y. Sharir, J. Pellog, and A. Grill, *Met. Technol.*, Vol 5, 1978, p 190
10. S.A. David and C.T. Liu, *Proc. Conf. on Grain Refinement in Castings and Welds*, G.J. Abbaschian and S.A. David, Ed., TWS-AIME, 1983, p 249-257
11. J.G. Garland, *Met. Constr. Br. Weld. J.*, Vol 6, 1974, p 121-127
12. F. Matsuda, H. Nakagawa, K. Nakata, and R. Ayani, *Trans. Jpn. Weld. Res. Inst.*, Vol 7, 1978, p 111-127
13. F. Matsuda, K. Nakata, Y. Miyanaga, T. Kayano, and K. Tsukamoto, *Trans. Jpn. Weld. Res. Inst.*, Vol 7, 1979, p 33-45
14. G.M. Reddy, A.A. Gokhale, and K. Prasad Rao, *J. Mater. Sci.*, Vol 32, 1997, p 4117-4126
15. S. Kou and Y. Le, *Metall. Trans. A*, Vol 16, 1985, p 1345-1352
16. B.P. Pearce and H.W. Kerr, *Metall. Trans. B*, Vol 12, 1981, p 479-486
17. R. DeNale and W.E. Lukens, *Proc. of Ti-6211 Basic Research Programme, Second Conference*, B.B. Rath, B.A. MacDonald, and O.P. Arora, Ed., Office of Naval Research, Arlington, VA, 1984, p 203-228
18. S. Kou and Y. Le, *Metall. Trans. A*, Vol 16, 1985, p 1887-1896
19. R.P. Martukanitz, C.A. Natalie, and J.O. Knoefel, *J. Met.*, Vol 39, 1987, p 38-42
20. A. Gutierrez, J.C. Lippold, and W. Lin, *Mater. Sci. Forum*, Vol 217-222, 1996, p 1691-1696
21. T.H. Courtney, *Mechanical Behaviour of Materials*, McGraw-Hill, 1990, p 171
22. D.M. Bowden and P.J. Meschter, *Scr. Metall.*, Vol 18, 1984, p 963-968
23. M.J. Dvornak, R.H. Frost, and D.L. Olson, *Weld. J.*, Vol 68, 1989, p 327s-335s